Results from HHFW System Operation on NSTX*

D. W. Swain[a], J. R. Wilson[b], P. M. Ryan[a], J. B. Wilgen[a], J. Hosea[b], M. D. Carter[a], and the NSTX Team

[a]*Oak Ridge National Laboratory*
[b]*Princeton Plasma Physics Laboratory*

Abstract. The HHFW system on NSTX has operated with the full 12-antenna, 6-transmitter configuration, delivering over 2 MW reliably for pulse lengths over 100 ms with various phasings of the antenna system. A circuit model of the full 12-antenna coupled system has been developed that gives good agreement with vacuum measurements. When it is used to extract the effects of the plasma on the rf circuit, pronounced asymmetries in antenna loading are observed, even when antenna phasing is symmetrical (e.g., 0π0π0π…..). The loading of the plasma on the antenna has been calculated with the RANT3D code using measured edge density profiles in front of the antenna ; these agree with measured loading values.

Recent progress has been made in the operation of the high-harmonic fast wave (HHFW) system on NSTX [1,2,3]. Figure 1 shows a 1.8 MW rf pulse (≈ 300 kW from each of six rf sources) fired into a plasma with current increasing to 1 MA. The antenna consists of twelve current straps in six resonant loops, the first loop containing straps 1 and 6, the second 2 and 7, etc. [4,5]. The phase of the rf sources relative to the first one, shown at the right of the Fig. 1, indicates that the "ideal" phasing of 0π0π0π was not achieved. The relatively small departure from ideal phasing will be shown to make a significant difference in the rf system characteristics.

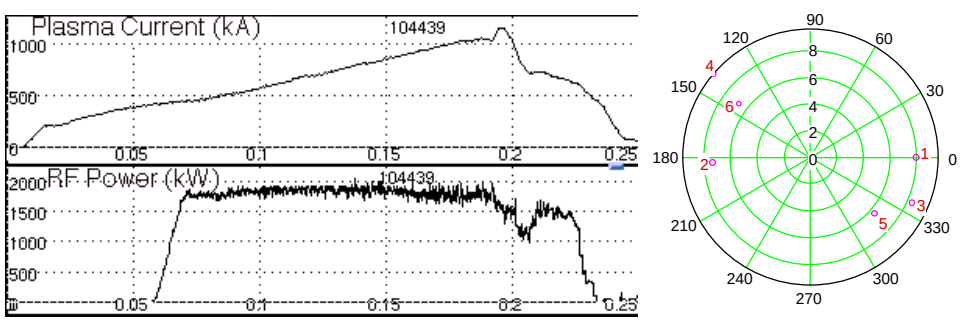

FIGURE 1. Plasma current and RF power for shot 104439 (left), and phase of the six rf sources relative to source 1 during the rf pulse (right).

* This research was sponsored by the Office of Fusion Energy, U. S. Department of Energy, under contract DE-AC05-00OR22725 with Oak Ridge National Laboratory managed by UT-Battelle and under contract DE-AC02-76CH03073 with Princeton Plasma Physics Laboratory.

A circuit model of the rf system was made that contains the current straps with mutual inductive coupling. In the usual model, plasma loading is modeled with a uniform loading R' (ohms/m) along each strap to account for the losses in the plasma. This model can also be used to analyze measured forward and reflected power on each line to yield an experimentally measured loading R'(t); we define the experimental value of R' to be the value that would give the experimentally measured forward and reflected powers if it were used in an *uncoupled* model of a resonant loop with current straps at both ends. Values of R'(t) determined in this manner for each of the six resonant loops are plotted in Fig. 2 for the same shot as in Fig. 1. Also plotted is the outer gap, which is the distance between the outermost closed flux surface and the front of the HHFW antenna Faraday shields. Although there is a pronounced change in the gap during the shot, no significant change in loading is observed.

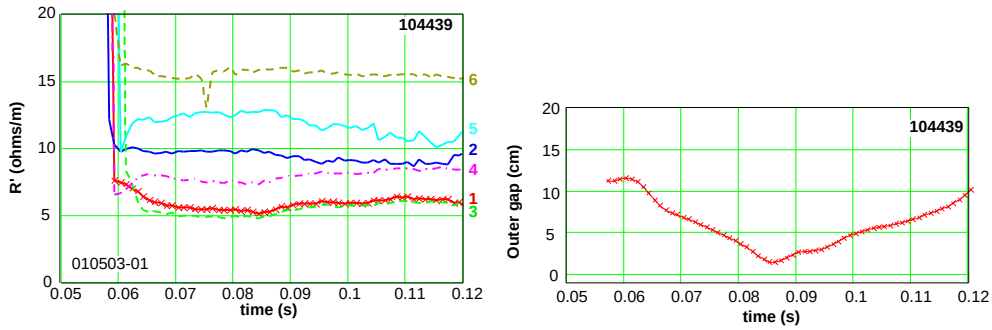

FIGURE 2. R'(t) for shot 104439 for each of the six rf sources (left), and outer gap (t) (right).

Figure 3 shows edge density profiles measured at four times during the shot by a microwave reflectometer. The density at which propagation begins for the dominant launched k_z of 14 m^{-1} (shown by the horizontal line) is almost always within a few cm of the Faraday shield, resulting in good coupling to the plasma.

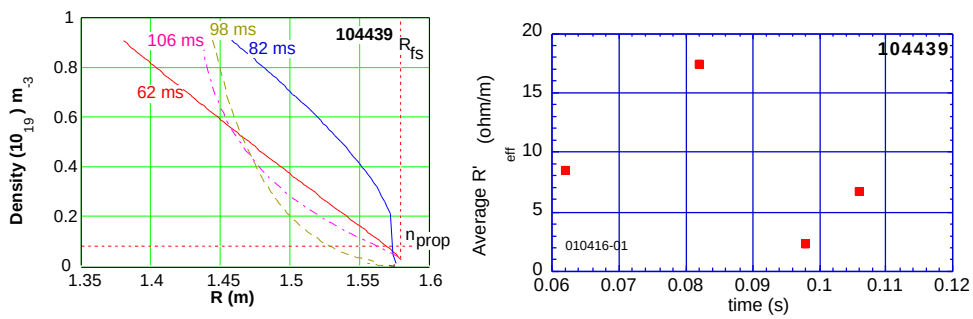

FIGURE 3. Edge density profile at four times in the rf pulse (left), and corresponding average values of R' from RANT3D (right), assuming the density profile is uniform in front of the antenna.

Observation of visible light from the edge also shows a fast density fluctuation, in filaments aligned along the magnetic field [6]. The loading computed using the RANT3D code [7] with each of these density profiles is significantly different from each other (see Fig. 3, right side). We believe that the antenna's large spatial extent averages out the measured fluctuations, thereby resulting in the fairly uniform loading in time shown in Fig. 2.

The question remains as to why there is about the factor of three difference in the loading measured on the different loops. This is explained by the coupled-circuit analysis of the system.

The coupled circuit equations of the 12-strap antenna system are

$$\frac{d\mathbf{V}}{dx} = \mathbf{Z'}\,\mathbf{I} \quad \text{and} \quad \frac{d\mathbf{I}}{dx} = \mathbf{Y'}\,\mathbf{V} \tag{1}$$

where **V** and **I** are the 12-element vectors of voltage and current, respectively, along the 12 coupled antenna straps, and **Z'** and **Y'** are 12x12 impedance and admittance matrices. In the usual model $Z'_{ij} = R'_i\delta_{ij} + j\omega M'_{ij}$, where R'_i is the (diagonal) load resistance value for loop i and M' is the inductance matrix. For the NSTX antennas, which have separate Faraday shields around each current strap, the **Y'** matrix is approximated as diagonal with the same values of capacitance (i.e., we set $Y'_{ij} = \delta_{ij}\, j\omega C'$), which is dominated by the strap-Faraday shield capacitance.

The left side of Fig. 4 is a plot of the measured values of Im(Z') for the 12x12 matrix with no plasma present. The right side of Fig. 4 shows the Z' matrix computed using RANT3D with the 62-ms density profile of Fig. 3. The nearest-neighbor terms have been reduced significantly from the vacuum values, and a pronounced asymmetry has been introduced by the plasma, causing some values to be negative.

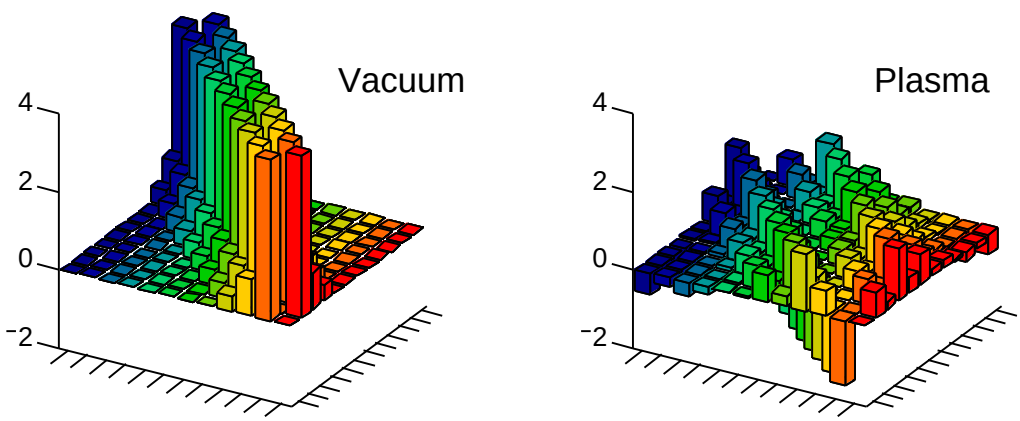

FIGURE 4. Imaginary part of 12x12 Z' matrix for antennas in vacuum (left) and with plasma (right) Diagonal elements (≈ 50 ohms/m) have been set equal to zero to show off-diagonal elements better.

These results appear to explain the pronounced asymmetries observed in R', as shown in Fig. 5. The solid curve in the left plot shows the measured values of R' from Fig. 2 (averaged from 80 to 120 ms) as a function of source number. The dashed curves are R' computed using RANT3D for the density profiles shown in Fig. 3. As can be seen, the R' values for the 62 and 106 ms density profiles (which are probably near the average density profile) are in reasonable agreement with the measured R' values. The right side of Fig. 5 shows the measured values compared to values calculated using the usual model for Z'. One of the curves is calculated with the vacuum values for inter-strap mutual inductances; the other is calculated with inter-strap coupling reduced to zero, to see if simply reducing the inter-strap coupling but not introducing any asymmetries into the Z matrix will give a match to the data. The results show that, while the reduced-coupling calculation does give improved

agreement with the measurements, the results using the full RANT3D Z matrix are better.

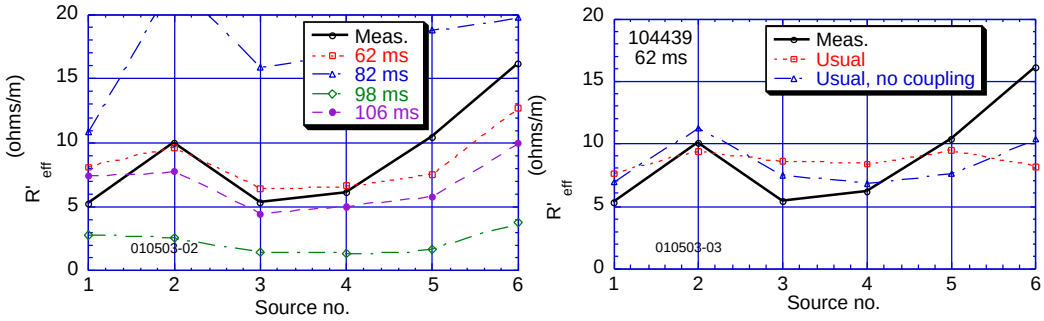

FIGURE 5. R' vs source number as measured (solid) and as calculated (dashed lines) for the four density profiles shown in Fig. 3. Left plot is RANT3D results; right plot is usual model.

CONCLUSIONS

The NSTX HHFW system is fully operational and has routinely delivered over 2 MW to the plasma. Measured density profiles in front of the antenna are observed to have large, localized fluctuations. It appears that the large spatial extent of the antenna array smoothes out the effects of localized fluctuations, so that the rf system sees a fairly constant loading with time. Relatively high edge densities usually allow the launched HHFW wave to begin propagating in the plasma only a few cm from the antenna, resulting in relatively high loading values for the antennas.

We observe significant asymmetry of loading on the rf system. This asymmetry appears to be quantitatively explained by the Z matrix calculations from RANT3D, when used in a coupled-circuit model of the rf system. Conventional coupled-circuit modeling that does not include the asymmetries in the antenna impedance matrix caused by the large poloidal field does not give as good agreement with the measurements as results using the full Z-matrix.

REFERENCES

1 B. P.LeBlanc, et al., "High-Harmonic Fast-Wave Heating in NSTX", this conference.
2 J. R. Wilson et al., "Plasma Response to the Application of 30 MHz RF Power in the NSTX Device", this conference.
3 J. E. Menard et al., "Pressure and Current Profile Modification Using Early High-Harmonic Fast Wave Injection in NSTX", this conference.
4 Wilson, J. R. et al., "High Harmonic Fast Wave Heating Experiments on NSTX", in *Proc. of 18th IAEA Conf. on Fusion Energy*, Sorrento, October 2000 (to be published).
5 D. W. Swain et al., "Results of High-Harmonic Fast Wave Experiments on NSTX", in *Proc. 27th EPS Conference on Contr. Fusion and Plasma Phys.*, Budapest, 12-16 June 2000, edited by K. Szego, T. N. Todd, S. Zoletnik, ECA Vol. 24B (2000) 808-811.
6 Maqueda, R. J. et al., *Rev. Sci. Instr.* **72**, 931-934 (2001).
7 Carter, M. D. et al., *Nuclear Fusion* **36**, 209 (1996).